The Angular and Spectral Kernel-Driven Model: Assessment and Application

Dongqin You, Jianguang Wen, Qiang Liu, Qinhuo Liu, *Member, IEEE*, and Yong Tang

***Abstract*—Land surface albedo is a critical parameter in the earth's energy budget. Multiple-sensor data contain more information than single-sensor data, enabling us to retrieve albedo more accurately. The Angular and Spectral Kernel driven model (ASK model), which introduces component spectra into a kernel-driven model, provides a way to combine multiple-sensor data to retrieve BRDF/albedo. The construction of the ASK model is detailed in Liu's paper. As a follow-up, this paper provides an extensive assessment of the ASK model and its application using multi-sensory data. The assessment is described in both angular and spectral dimensions using simulated datasets from ProSail, 5-Scale, and RGM. With the ability to combine information from the spectral and angular domains, the inversion of the ASK model requires fewer angular observations than the traditional model. Four angles are sufficient when combining seven MODIS bands. In the spectral dimension, the model performance reveals high numerical correlations among bands: the red and NIR bands are generally required to make a good spectra fitting, and adding an additional SWIR band can improve the performance. The synergistic retrieval of albedo combining FY3/VIRR, AVHRR, and MODIS shows a satisfactory agreement with *in situ* measurements, where the RMSE is 0.013 in the 4-day composited temporal resolution retrieval. The results show that the ASK model is promising for BRDF/albedo inversion using multi-sensor data, although it shows some dependence on the accuracy of the component spectra.**

***Index Terms*—Albedo, BRDF, angular and spectral model, multi-sensor.**

I. Introduction

LAND surface albedo, defined as the ratio of the upwelling radiative flux over land surface to the downwelling radiative flux [1], is a key parameter for energy budgets, climate forecasting, and global change predictions [2]–[5]. Albedo is usually derived from land surface reflectance by angular and spectral integration and thus depends on the land surface bidirectional reflectance distribution function (BRDF) [6]. The BRDF describes the land surface reflectance properties in terms of spectral, directional, spatial, and temporal characteristics [7], and allows a more accurate specification of land surface albedo derived from satellite remote sensing data [8], [9].

The available land surface BRDF/albedo products from remote sensing sensors, such as Moderate Resolution Imaging Spectroradiometer (MODIS) [10], [11], Polarization and Directionality of the Earth's Reflectances (POLDER) [12], [13], Meteosat Second Generation/Spinning Enhanced Visible and Infrared Imager radiometer (MSG/SEVIRI) [14], Advanced Very High Resolution Radiometer (AVHRR) [15] and Satellite Pour l'Observation de la Terre Vegetation (SPOT VEGETATION) [15], [16], are mainly generated from kernel-driven models, using multi-angular bidirectional reflectance in clear skies to invert the BRDF parameters. The multi-angular bidirectional reflectance is accumulated by multi-day revisits (e.g., 16 days or 10 days) of the same target observed from a single sensor. Coarse temporal resolution, deficient angular samplings, and limited spectral samplings are the challenge factors for albedo calculation.

Integrating multi-sensor (e.g., MODIS, AVHRR, and FengYun3/Visible and Infra-Red Radiometer (FY3/VIRR)) remote sensing data can provide more information about the land surface anisotropy, more spectral bands, and higher temporal resolution. This method improves the characterization of land surface properties in terms of fine spatial-temporal resolution and higher accuracy. However, challenges remain in the synergistic inversion with multi-sensor reflectance, including the differences in spectral response, spatial resolution, and spatial geometric match [17]–[19]. The angular and spectral kernel-driven model (ASK model) [20] presents a possible way for combining multi-sensor remote sensing data to synergistically retrieve BRDF/albedo. Developed from the kernel-driven model by introducing a new parameter of sensor-specific component spectra, it decouples the radiometric and structural parameters in the coefficients of the original kernel-driven model and adds a radiometric variable to the kernel functions. Thus, the new coefficients are spectral-invariant, which enables them be inverted by combining observations from different spectral channels.

The ASK model, derived in a previous paper [20], is promising for land surface BRDF and albedo inversion. However, further quantitative analysis still must be performed to investigate the performance of ASK on the angular and spectral features. This paper, as a part of Liu's series, presents

Manuscript received January 31, 2013; revised April 24, 2013; accepted May 16, 2013. Date of publication July 10, 2013; date of current version April 18, 2014. This work was supported by the National Natural Science Foundation of China (41271368, 91025006, 40901181), the National High Technology Research and Development Program of China (Grant 2012AA12A304, 2009AA122100) and EU Seventh Framework Program (CEOP-AEGIS). *(Corresponding author: J. Wen.)*

D. You is with the State Key Laboratory of Remote Sensing Science, jointly sponsored by the Institute of Remote Sensing and Digital Earth of Chinese Academy of Sciences and Beijing Normal University, Beijing 100101, China, and also with University of Chinese Academy of Sciences, Beijing 100049, China. (e-mail: youdongqin@gmail.com).

J. Wen, Q. Liu, Q. Liu, and Y. Tang are with the State Key Laboratory of Remote Sensing Science, jointly sponsored by the Institute of Remote Sensing and Digital Earth of Chinese Academy of Sciences and Beijing Normal University, Beijing 100101, China (e-mail: wenjg@irsa.ac.cn, liuqiang@irsa.ac.cn, qhliu@irsa.ac.cn, tangyong@163.com).

Color versions of one or more of the figures in this paper are available online at http://ieeexplore.ieee.org.

Digital Object Identifier 10.1109/JSTARS.2013.2271502

the assessment of the robustness of the ASK model in BRDF inversion and its application using multi-sensor data.

II. Angular and Spectral Kernel-Driven Model

The ASK model is developed from the kernel-driven model. Using the prior knowledge of the component spectra, the spectral variable is extracted from the original kernel coefficients and integrated into the kernels. The model is expressed as (1).

$$\begin{aligned} R(\theta_i,\theta_v,\phi,\lambda) &= c_1k_1(\lambda)+c_2k_2(\lambda)+c_3k_3(\theta_i,\theta_v,\phi,\lambda) \\ &\quad + c_4k_4(\theta_i,\theta_v,\phi,\lambda)+c_5k_5(\theta_i,\theta_v,\phi,\lambda) \end{aligned} \tag{1}$$

$$k_1(\lambda) = \frac{1}{\pi}\rho_g(m_0,\lambda)$$

$$k_2(\lambda) = -\frac{1}{\pi}A_w(\lambda)\cdot\rho_g(m_0,\lambda)$$

$$k_3(\theta_i,\theta_v,\phi,\lambda) = \frac{2}{3\pi}\rho_c(\lambda)\cdot\left(k^c_{\text{geo}}+1\right)+\frac{1}{\pi}k^g_{\text{geo}}\cdot\rho_g(m_0,\lambda)$$

$$k_4(\theta_i,\theta_v,\phi,\lambda) = -\frac{1}{\pi}k^g_{\text{geo}}\cdot A_w(\lambda)\cdot\rho_g(m_0,\lambda)$$

$$\begin{aligned} k_5(\theta_i,\theta_v,\phi,\lambda) &= \frac{2}{3\pi^2}\rho_c(\lambda)\cdot k^\rho_{\text{vol}}+\frac{2}{3\pi^2}\tau_c(\lambda)\cdot k^\tau_{\text{vol}} \\ &\quad + \frac{1}{3\pi}\rho_c(\lambda)+\frac{1-\sqrt{1-w(\lambda)}}{\pi(1+2\cos(\theta_i)\sqrt{1-w(\lambda)})} \end{aligned}$$

$$\begin{aligned} c_1 &= a_1\cdot(1-n\pi r^2)+a_2\cdot\exp(-bF) \\ c_2 &= a_1\cdot(1-n\pi r^2)\cdot(m_1-m_0) \\ &\quad + a_2\cdot\exp(-bF)\cdot(m_2-m_0) \\ c_3 &= a_1\cdot n\pi r^2 \\ c_4 &= a_1\cdot n\pi r^2\cdot(m_1-m_0) \\ c_5 &= a_2\cdot(1-\exp(-bF)) \end{aligned}$$

where $k_1 \sim k_5$ are the reconstructed kernels, kernel k_1 is an isotropic term, k_3 is a geometric term, and k_5 a volumetric term corresponding to the original kernel-driven model. Including the soil moisture and the multi-scattering in the equation (i.e., k_2 and k_4, respectively) improves the ASK model's accuracy. k^g_{geo} and k^c_{geo} are the ground and canopy parts in the Li-sparse kernel, and k^ρ_{vol} and k^τ_{vol} are the reflectance and transmittance terms in the Ross-thick kernel. $c_1 \sim c_5$ denote the five kernel coefficients, which are independent of the sensor and band. The component spectral parameters, i.e., leaf reflectance $\rho_c(\lambda)$, leaf transmittance $\tau_c(\lambda)$, soil reflectance $\rho_g(\lambda)$, soil moisture attenuating factor $\mathrm{A}\omega(\lambda)$, are band-specific and collected beforehand. In this paper, the soil moisture factor $\mathrm{A}\omega(\lambda)$ is from laboratory experiment [21]. The sensor-specific band spectral response functions and the typical component hyper-spectra are used to derive the ASK component spectral parameters.

$$CS_{mn} = \frac{\int_{\lambda_1}^{\lambda_2} r(\lambda)\cdot B_{mn}(\lambda)d\lambda}{\int_{\lambda_1}^{\lambda_2} B_{mn}(\lambda)d\lambda} \tag{2}$$

CS_{mn} is the predetermined sensor-depended component spectral parameter for sensor m and band n, and $r(\lambda)$ is the continuous component spectral parameters measured in the laboratory. $B_{mn}(\lambda)$ is the response of the spectral channel specified by sensor m and band number n.

III. Assessment of ASK Model Performance

According to (1), the kernel k_i is a function of the component spectra and the illumination-viewing geometry, while the coefficient c_i depends on the land surface structural parameters which can be inverted by multi-band and multi-angle reflectance data. The quality of the component spectra input as priori-knowledge, the angular samplings of the reflectance data and the spectral information of the reflectance data are the three important elements in ASK land surface BRDF/albedo inversion. This section presents an assessment of the effects of the component spectra and the performance of BRDF inversion in angular and spectral dimensions.

A. Simulated Datasets

To prevent the influence of unknown noise in actual satellite data, simulated BRF datasets are used to assess the ASK model. Three models are selected to simulate BRFs of different vegetation canopies: the ProSail model [22], [23], 5-Scale model [24], [25] and RGM model [26]. ProSail couples the PROSPECT model to simulate the broad leaf spectra and the SAIL model to obtain the canopy BRFs. 5-Scale combines the LIBRTTY model to simulate the pine leaf spectra and the 4-Scale model to obtain the canopy BRFs. RGM models the BRFs by simulating realistic crop structure and light propagation. Each model uses the same set of component spectra (leaf and soil spectra) as input, whereas the canopy structures are depicted using three different sets of structural variables. The LAI is varied from low to high to simulate nearly bare to well-vegetated areas. For ProSail and 5-Scale, the canopy reflectances are simulated under 32 actual MODIS (both Terra and Aqua) observation geometries extracted from a pixel during a 16-day cycle and then integrated with the 7 spectral response functions of the MODIS optical bands to derive the MODIS-like BRF, where the center wavelengths from Band1 to Band7 are 0.648 μm, 0.858 μm, 0.470 μm, 0.555 μm, 1.240 μm, 1.640 μm, and 2.13 μm respectively [27]. In the RGM model, MODIS red and NIR bands are simulated under 75 observation geometries distributed in three observing planes. The main parameters for each model are listed in the tables (Tables I, II, and III), some examples of the simulated reflectance are shown in Fig. 1.

B. Assessment of the Effects of the Component Spectra

The component spectra are a special feature of the ASK, affecting the reconstructed kernels rather than the original ones. The characters of the kernel shapes vary with the component spectra. Another issue is the uncertainty caused by the component spectra with errors to the albedo retrieved by the ASK.

1) Character of the Kernel Shapes: The geometric-optical (geo) term Li-sparse kernel and the volume scattering (vol) term Ross-thick kernel are selected to investigate the effect of the component spectra on the kernels. The ASK kernels are presented in a two-dimensional feature space: angular and spectral dimensions. The shapes are drawn along principal planes with three solar zenith angles: 0°, 30°, 60°. The input component spectra are the broad leaf (simulated by the Prospect model)

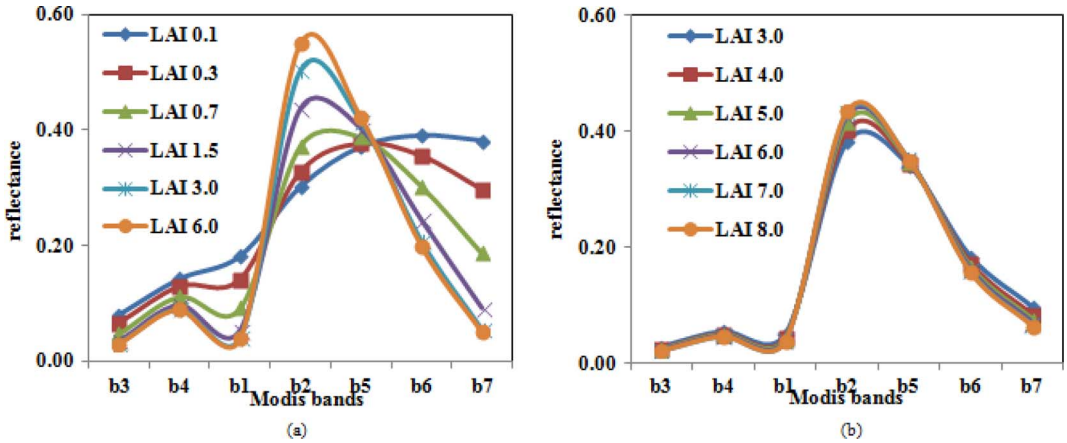

Fig. 1. Canopy reflectance with different LAIs in the observation geometry with a sun zenith angle of 40.56°, view zenith angle of 60.41° and relative azimuth angle of 38.72°. (a) is ProSail, (b) is 5-Scale.

TABLE I
PROSAIL MODEL PARAMETERS

Parameter	Values
Component spectra	Leaf spectra simulated by Prospect model Soil spectra measured in field
Diffuse skylight factor	0.1
Three major sets of structural parameters (leaf angle distribution)	Custom, uniform, spherical
LAI	0.1, 0.3, 0.7, 1.5, 3.0, 6.0
Illumination-view geometry	MODIS observation geometry

TABLE II
5-SCALE MODEL PARAMETERS

Parameter	Values
Component spectra	Leaf spectra simulated by LIBERTY model Soil spectra measured in field
Diffuse sky light factor	0.1
Three major sets of structural parameters (GE_CHOICE, SHAPE, Ha(m), Hb(m), B(m2), D, m2, OMEGA_E)	Set 1: NO_BRANCH, SPHEROID, 10.0, 7.0, 10000,1000, 2, 0.98 Set 2: BRANCH, cone&cylinder, 3, 10, 10000,4000, 4, 0.80 Set 3: BRANCH, cone&cylinder, 1, 10, 10000,2000, 8, 0.5
LAI	3, 4, 5, 6, 7, 8
Illumination-view geometry	MODIS observation geometry

Parameters:Ha—height of the lower part of the tree,Hb—height of cylinders, B-domain size,D—Number of trees in the domain,m_2—cluster mean size, OMEGA_E—clumping index for shoots

TABLE III
RGM PARAMETERS

Parameters	Values
Component spectra	Leaf reflectance in red and NIR: 0.079, 0.431 Leaf transmittance in red and NIR: 0.036, 0.530 Soil reflectance in red and NIR: 0.163, 0.209
Diffuse skylight factor	0.12
Three major sets of row structural parameters (row height, row width and row gap width, row width)	Set 1: 20 cm, 100 cm, 50 cm Set 2: 30 cm, 100 cm, 50 cm Set 3: 40 cm, 100 cm, 50 cm
LAI	0.5, 1.5, 3, 4.5
Illumination-view geometry	Solar zenith and azimuth angle: 22.12°, 135.32° View zenith angle: from 0° to 65° in a 5° interval View azimuth (3 planes): 135°\315°, 45°\225°, 0°\180°

and needle leaf (simulated by the Liberty model) spectra, the field-measured soil spectra, and laboratory-measured soil absorption factor. All the spectra are integrated with MODIS red and NIR band spectral responses, which capture the major features of vegetated areas.

Figs. 2 and 3 show that the reconstructed kernels have retained the general shapes of the original kernels. The new geometric optical kernels present hot-spot effects, taking the shape of bells, when characterizing the shadow and sunlight in the scene. The new volume scattering kernels present the bowl effect to describe the radiative transfer through horizontal homogeneous media. The ASK kernels strongly reflect the BRDF angular characteristics from the original kernels.

The new kernels not only characterize the angular effect but also present the spectral features. Comparing the three subfigures (g), (h), (i) in Fig. 2, both the needle and broad leaf geometric-optical kernels in the red band (Fig. 2(g)) in large view zenith angles at the backscattering decline, whereas the kernel in NIR (Fig. 2(h)) retains the original (Fig. 2(i)) trend. The kernels also vary by species. As shown in Fig. 2(e), the needle leaf changes the original kernel shape, whereas the broad leaf is similar to the original kernel shape in the NIR band. These phenomena also appeared in the volumetric scattering kernel. The difference in the component spectra accounts for these shape changes as the component spectra varies from vegetation species, soil types, and spectral regions.

Compared with the vol-kernel, the shape of the ASK geo-kernel changes more dramatically from the original geo-kernel, as shown in Figs. 2 and 3. In the original vol-kernel, the reflectance and the transmission of the leaf are assumed to be the same. In the ASK vol-kernel, the reflected and transmitted parts are considered separately. Nevertheless, this assumption causes only slight distortions because the leaf reflectance and the leaf transmittance are very similar over the entire spectrum. However, for the geo-kernel, the sunlit canopy and sunlit ground show very different shapes in the original kernel, as shown in

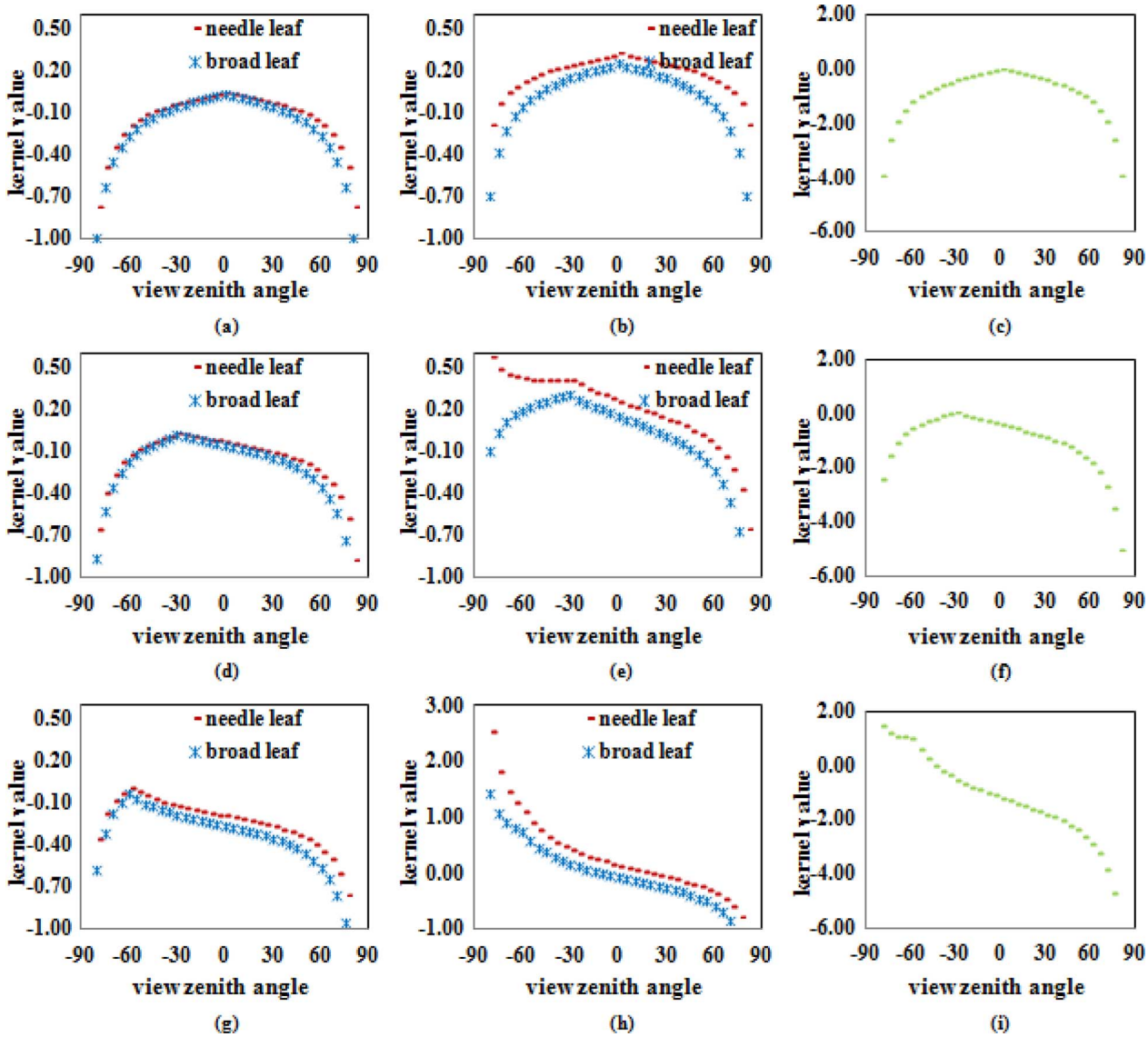

Fig. 2. Geometric optical kernel shape along principle plane. The sun zenith angles from the first row to the third row are 0°, 30°, and 60°; the three columns from left to right are the ASK kernel in MODIS band1, ASK kernel in MODIS band2, and original kernel. Positive (negative) view zenith angles refer to forward (backward) scattering.

Fig. 4. Additionally, the two components have very different spectral features. Thus, the geo-kernels are more varied.

2) Uncertainty From the Component Spectra: To investigate the uncertainty caused by the inaccurate component spectra (leaf reflectance, leaf transmittance and soil reflectance), three types of errors are taken into consideration. For the first type of error, random noises (5%, 10%, 15%, and 20% normally distributed random noises) are added to the true component spectra used in the BRF datasets constructions, accounting for the disturbance of spectra caused by measurement errors and the temporal and spatial variance of the same land type of leaf or soil. For the second type of error, different types of component spectra (e.g., leaf component spectra of 45 leaf samples obtained from trees, crops, and plants provided by the Leaf Optical Properties Experiment 93 (LOPEX93) [28] and 25 samples of soil spectra obtained from the Johns Hopkins University spectral library are input, accounting for the cases of incorrect knowledge of vegetation species and soil types. Finally, the leaf transmittance is replaced by leaf reflectance to assess the uncertainty from the assumption that the leaf transmittance is equivalent to the leaf reflectance.

Besides the uncertainty in component spectral parameters, the reflectances in the inversion are supplemented with 0.01 random errors. The reflectance from all seven bands is combined, and 4 angles are randomly chosen from the simulated BRFs to retrieve the ASK coefficients. Then, the coefficients and the corresponding component spectra are used to integrate the shortwave BSA and WSA, which will be compared with the values calculated by the accurate component spectral parameters.

Figs. 5 and 6 show the statistics of the albedo retrieved for different component spectra errors. The WSA provides a similar result to the BSA because the former is the BSA integration over sun angle. Therefore, the analysis below focuses on the BSA.

The retrieved albedo of the first type of errors are nearly normally distributed around the true albedo of each BRF dataset. The bias increases with the magnitude of noise in the compo-

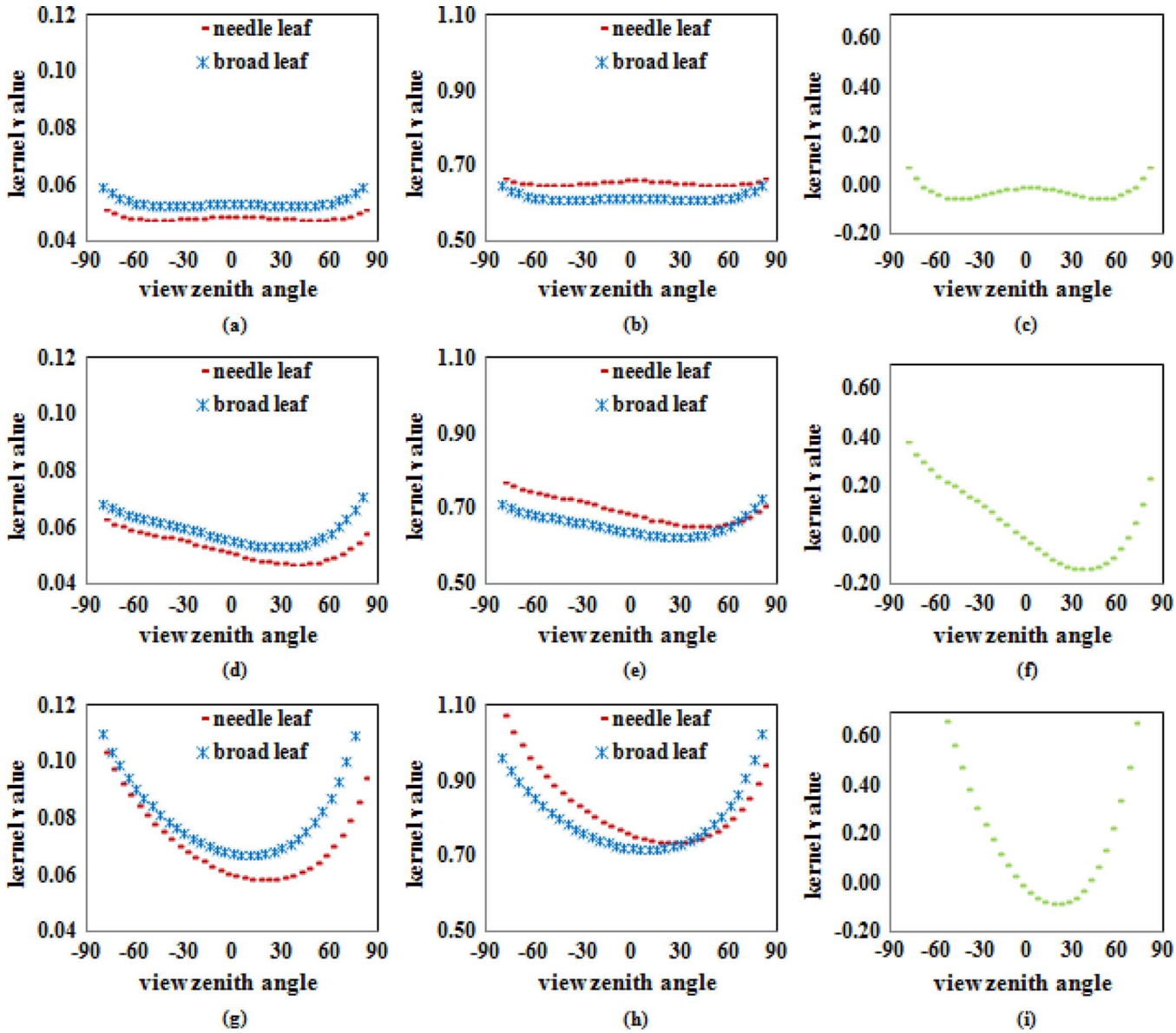

Fig. 3. Volume-scattering kernel shape along principle plane. The sun zenith angles are 0°, 30°, 60° from first row to the third row, respectively; the three columns from left to right are ASK kernel in MODIS band1, ASK kernel in MODIS band2, Original kernel separately. Positive (negative) view zenith angles refer to forward (backward) scattering.

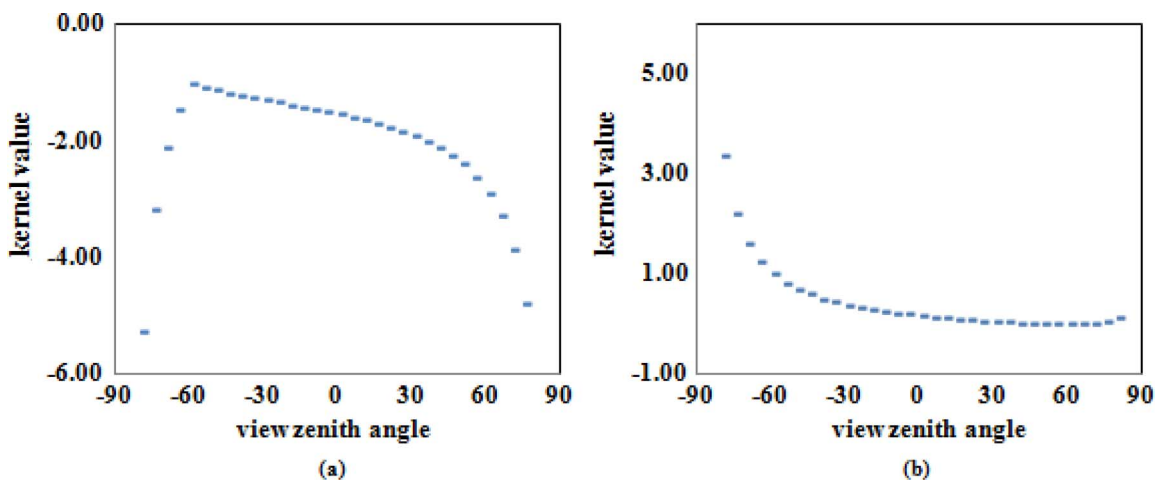

Fig. 4. The two parts of the original geometric-optical kernel when the sun zenith angle is 60°: (a) sunlit ground, (b) sunlit canopy.

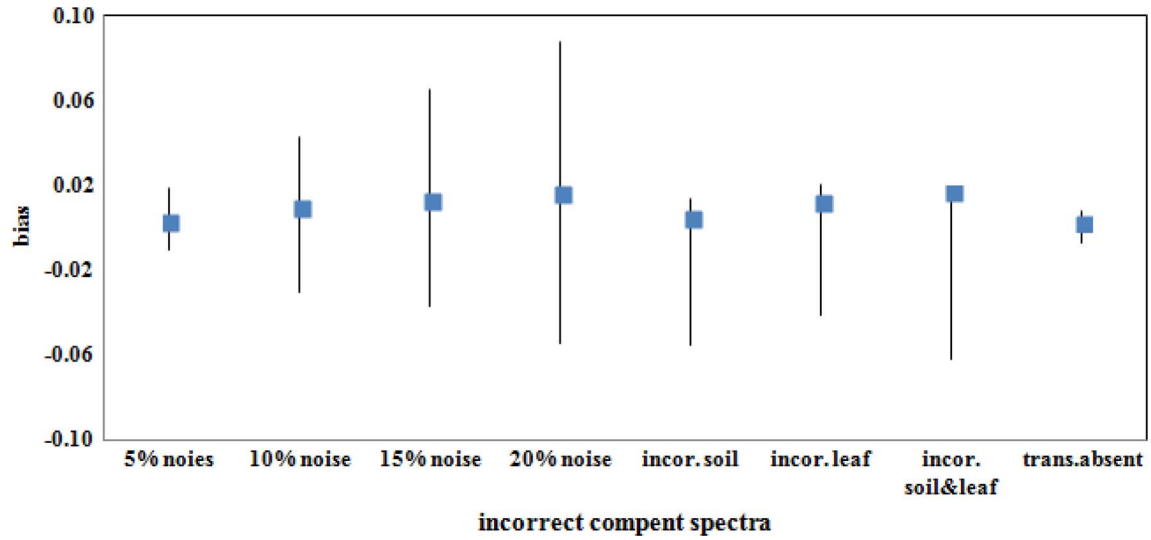

Fig. 5. Bias in retrieved BSA when using inaccurate component spectra. The squares are the average absolute bias, whereas the lines indicate the bias range. "incor." is shorted for "incorrect", "trans.absent" is the case that leaf transmittance is replaced by leaf reflectance.

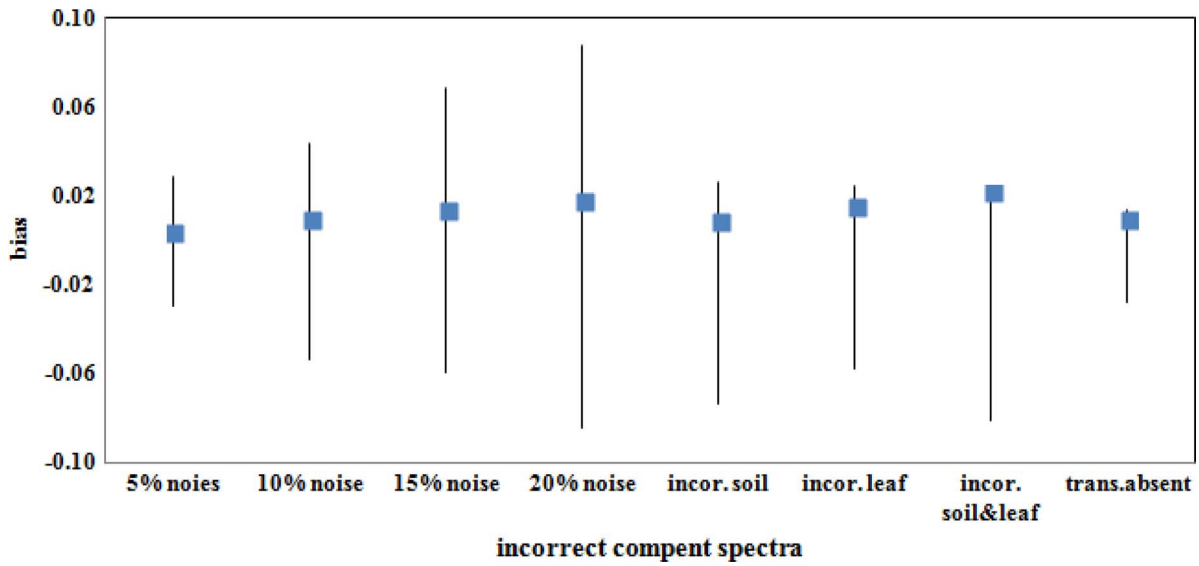

Fig. 6. Bias in retrieved WSA when using inaccurate component spectra. The squares are the average absolute bias, whereas the lines indicate the bias range. "incor." is shorted for "incorrect", "trans.absent" is the case that leaf transmittance is replaced by leaf reflectance.

nent spectra. The errors are within 0.02 and 0.05 for 5% and 10% noise, respectively. The maximum bias, occurring for the 20% random noise, reaches 0.087. However, the average absolute errors of each level of random noise are fairly steady. The ASK is robust to the random noise in the component spectra when the noise levels are within 10%.

The ASK involves leaf and soil components; thus, ASK coefficient inversion with different component spectra is complicated. To assess the effects of the inaccuracy of the components in detail, three sub-situations are investigated: 1) incorrect soil spectra; 2) incorrect leaf spectra; 3) incorrect soil spectra and leaf spectra. Fig. 7 shows how the BSA changes with the component spectra for each BRF dataset.

The scenes with low LAI are more sensitive to soil spectra than those with high LAI (see Fig. 7(a)), whereas the scenes of high LAI are more sensitive to the leaf spectra (see Fig. 7(b)). In addition, the retrieved results based on the incorrect soil and leaf spectra exhibit higher uncertainty than the cases of only one incorrect component spectrum. When the component spectrum uncertainty is only derived from the soil, most of these albedo are very close to the true ones retrieved by accurate component spectra, with an average absolute error of 0.005. For the uncertainty from leaf spectra, except for several extreme cases, most of the retrieved albedo exhibit satisfactory accuracy precision, with an average absolute error of 0.012. The uncertainties from incorrect soil and leaf spectra are additive, with an average absolute error of 0.017.

When the leaf transmittance is absent and replaced by the leaf reflectance, the biases are mostly within 0.005 and the average absolute error is 0.007. Such a simplification (leaf transmittance equals leaf reflectance) for the ASK can satisfy the accuracy requirement and again proves that the separate calculation of the

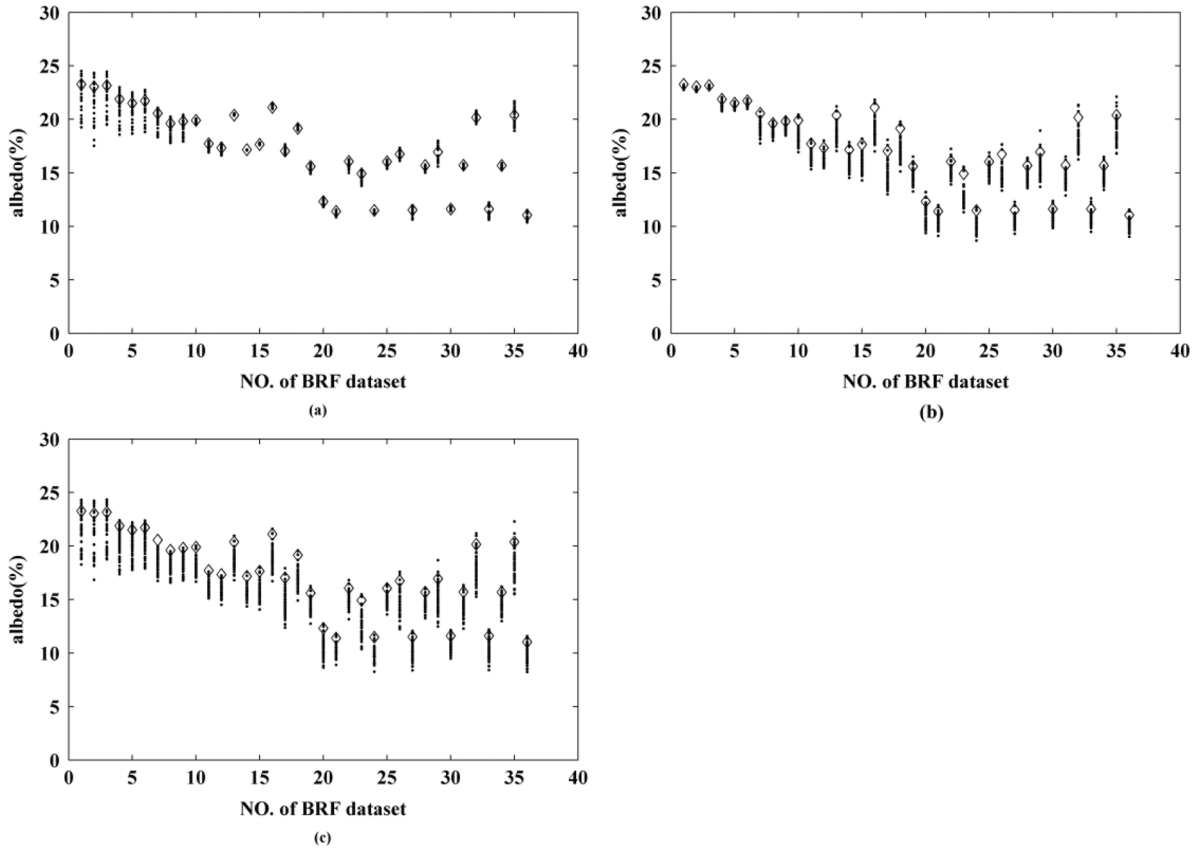

Fig. 7. BSA variation with component spectra for each BRF dataset. The BRF datasets from PROSAIL are numbered from 1–18, and every three datasets have the same LAI, taking values of 0.1, 0.3, 0.7, 1.5, 3.0, and 6.0 sequentially (i.e., the x values from 1 to 3 have a LAI of 0.1). The datasets from 5-Scale are numbered from 19–36, and every three datasets have the same LAI, ranging from 3 to 8 with a step of 1. The square symbol represents the true albedo, and the points indicate cases of inaccurate component spectra. (a) is incorrect soil spectra, (b) incorrect leaf spectra, (c) incorrect soil and leaf spectra.

leaf reflectance and transmittance in the ASK vol-kernel will not strongly change the original kernel.

In the cases of changing leaf spectra, most of the albedo results from such inaccurate leaf spectra are lower than the true values from accurate component spectra (Fig. 7(b) and (c)). This is due to the fact that most of the LOPEX spectra having higher values in SWIR than the spectra simulated by PROSPECT or LIBERTY, as shown in Fig. 8. All bands contribute equally to the retrieval, and the retrieved coefficients are a balance of all bands, minimizing the total residuals. When the spectra input are much higher than the exact values in band5, band6 and band7, the coefficients will be adjusted to fit the BRF. In this way, the coefficients that fit band5, band6 and band7 well will lower the VIS/NIR values. The retrieval results satisfy the BRF fitting requirements with the least total residuals. However, for the albedo calculation, the fitting residuals in the VIS/NIR will be amplified because the albedo integrated over the whole shortwave band has higher weight in the VIS/NIR than in the SWIR, leading to a lower broadband albedo.

C. Assessment of the BRDF Inversion in Angular and Spectral Spaces

With the new form of kernel functions, the ASK model can be inverted by combining multiple bands together, whereas the traditional kernel-driven model can only be inverted band-by-band. Thus, stable inversion can be obtained using fewer angular observations. For example, even if there is only one observation from MODIS, it is possible to combine the reflectance of 7 bands to compute the five coefficients of the ASK model. In contrast, for the traditional model, at least 3 observations are needed to invert the three spectral-dependent kernel coefficients.

Meanwhile, correlations exist between bands, the necessary combination of band reflectances for the robust inversion of the ASK model must be determined. Furthermore, the addition of more band observations into the inverse system not only increases the overall data information but also introduces additional uncertainties, which may have negative effects on the BRDF fitting ability or the broadband albedo retrieval. The ability of kernel-driven models to fit BRDF shapes has been demonstrated in previous studies [29]. Here, the data fitting and extrapolation of the ASK model in the angular and spectral domains are first analyzed separately by inverting the ASK model coefficients using different angular combinations under the standard band setting and different band combinations under the same geometric angle, respectively. Next, both the combination of bands and the number of angles are synchronously optimized to obtain the best inversion result under the practical limitations of satellite sensors.

1) Effects of the Angular Sampling in ASK BRDF Inversion: The effects of angular sampling on the ASK model and the original kernel-driven model are compared using the simulated BRF

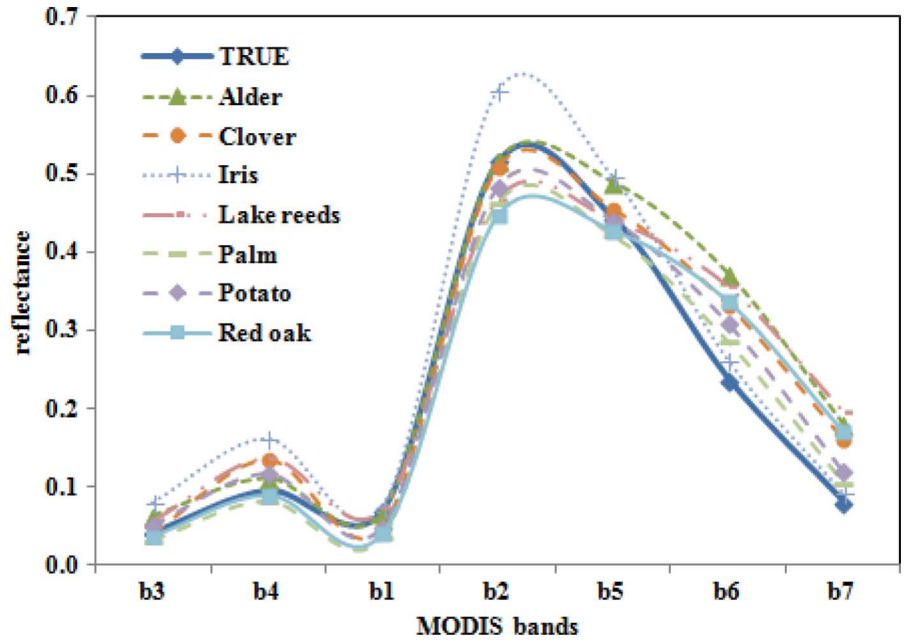

Fig. 8. Input leaf spectra ('TRUE' denotes the leaf spectra obtained from the 5-Scale model simulation of the BRF datasets; other data are the leaf spectra from LOPEX).

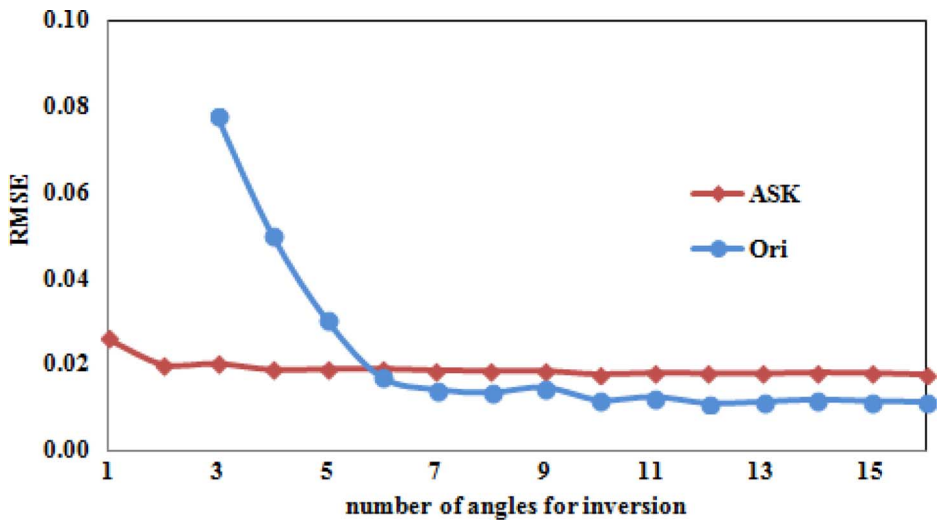

Fig. 9. RMSE of the BRF fitting retrieved by the ASK and original models with various numbers of angles.

datasets. For each dataset, several angular samplings are randomly chosen for inversion, and the remainders are used to validate the accuracy of the simulated BRF by the two models. The ASK model is inverted with 1 to 16 randomly chosen angles, combining all bands. In addition, the input ASK component spectra are the component spectra used in the simulation dataset. The original kernel-driven model (abbreviated as Ori) is inverted using 3 to 16 observations per band. The RMSE and R^2 are presented in Figs. 9 and 10.

As the number of observations in the inversion increases, both the ASK and original models achieve more stable inversions; however, ASK requires fewer observations to obtain stability. For sparse angular samplings (fewer than 7 observations), ASK is clearly advantageous. Even for fewer than 3 angle samplings, ASK can obtain acceptable results with an RMSE below 0.026 and an R^2 above 0.96. However, for the original model, it is impossible to solve the original model's three kernel coefficients. Even 3–6 observations are not enough to obtain stable inversion results, as the high RMSE values indicate the prediction failure of the original model. For ASK, when the angle number reaches 4, the RMSE is 0.0187. In addition, as the number of observations increases, the RMSE of ASK decreases below 0.001, leading to no obvious improvement in the inversion accuracy. Thus, four angles allows ASK to achieve full inversion. For the original model, the same conclusion is obtained as for the AMBRALS algorithm, i.e., that seven angle samplings are sufficient.

The RMSE and R^2 of the two models indicate that the original model performs slightly better in the angular prediction under the condition of full inversion, for which the average RMSE of

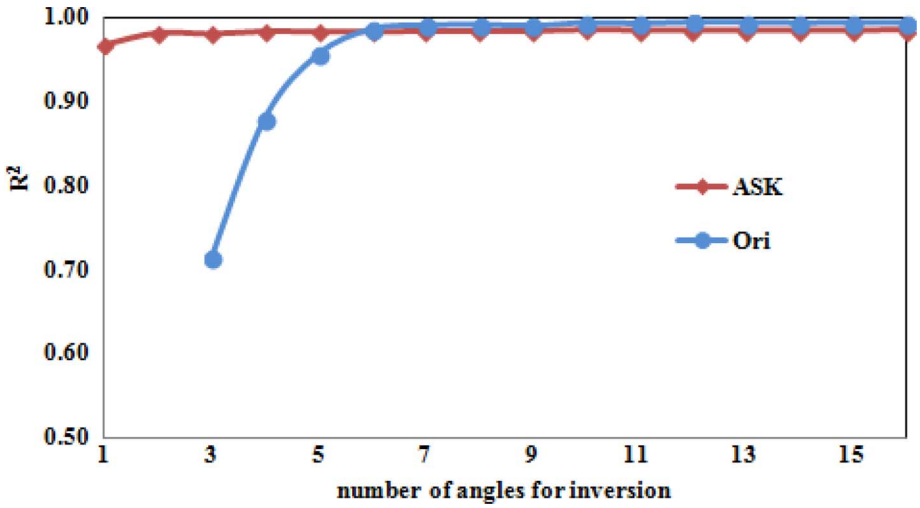

Fig. 10. R^2 of the BRF fitting with different number of angles retrieved by the ASK and original models.

the original model is 0.006 less than that of the ASK model. In both the backward inverting and forward modeling processes, ASK combines all bands to calculate one set of coefficients and apply the coefficients to all the bands, whereas the original model is inverted and fits the BRDF per band. Thus, ASK's inversion is the balance of all bands, which slightly decreases the total accuracy relative to the original model.

2) Effects of the Spectral Dimension in ASK BRDF Inversion: Almost all current VIS/NIR sensors have set red and NIR bands (like the 1st and 2nd MODIS band), which contain most of the vegetation information. In the ASK model, the variable m in coefficients C_2 and C_4 (seen (1)) accounts for the soil moisture. And the SWIR bands (like the 6th or 7th MODIS band) are sensible to the soil moisture. Therefore, the ASK model will be examined under various band combinations, such as band1, band2, band1+2, band1+2+7. A stable inversion requires the number of equations to be double the number of unknown variables in the functions. When only one band is used in the inversion, 11 angles are needed to calculate the ASK coefficients. To control the sources of uncertainty, all band combinations will be retrieved under the same observation geometries. In each situation, the remaining bands will be fitted by ASK in the same observation geometries. In this way, the only variable is the spectra when applying the coefficients to other bands to test ASK's prediction ability. The results are shown in Fig. 11 and Table IV.

Inversions with a single band1 or band2 are worse than inversions combining bands. When using only the band1 to invert the coefficients, the ASK model predictions are inaccurate for band2, band4, and band5, especially for band2, where the RMSE is 0.255. For the case of band2 inversion, the ASK model provides poor fits for almost all bands except band5; the RMSE for band1 and band7 reach 0.079 and 0.189, respectively, which are very high relative to the values of the bands. However, the results improve when band1 and band2 are incorporated. In addition, the introduction of band7 reflectance into the inversion equation contributes to the fitting of band5 and band6 reflectance.

These results indicate that the ASK performance in the spectral dimension shows very high numerical correlation among spectra. Here, we consider the fitting of band3, band4, band5, and band6, which are comparable in the four inversion situations. Band3 is a strong absorption band for vegetation with low values, similar to the band1. Its RMSE peaks at 0.042 when band1 is not used in the inversion. When band1 is added to the inversion, its RMSE remains near 0.005. Band4 is a small reflectance peak whose values are intermediate to band1 and band2. The fitting RMSE is approximately 0.014 when using band1 and band2 in the inversion, which is better than the results obtained using only band1 or band2 (0.026 and 0.0576, respectively). Band5 (1.2 μm) and band6 (1.6 μm) are reflectance peaks around the water absorption bands (1.4 μm). The values of band 5 are slightly higher than those of band6 near band2, and its highest fitting RMSE (0.174) is produced by the inversion excluding band2. Both band5 and band6 can achieve good fitting when the red and NIR bands are involved, and adding band7 can improve their predictions somewhat. These results show that ASK yields good predictions for the bands that are numerically close to the bands involved in the inversion.

3) Effects Involving the Angular and Spectral Dimensions in ASK BRDF Inversion: Based on Section III-C.2, band1 and band2 will be used, with other bands being added individually to the retrieval under different angular samplings. The R^2 values for the following fittings are very high (0.97–0.98) for all cases. However, the RMSE is a better indicator.

Fig. 12 presents selected cases of the combination of various numbers of bands, which are close to the best fittings among the same number of bands combined situations. Multiple bands combining inversion in ASK do require fewer angle samplings compared to the traditional kernel-driven model. Even in very poor angular samplings like 2 or 3 angles in each case of band combinations, the fittings are still acceptable with a change about 0.003 in the RMSE comparing to the full inversion. And for all these band combinations, 4 to 5 angles are needed for stable inversion.

Fig. 12 also shows that combining more bands decreases the RMSE, but different bands contribute differently. Here, we focused on three-band combinations (details shown in Fig. 13). When combining the red and NIR band only, the

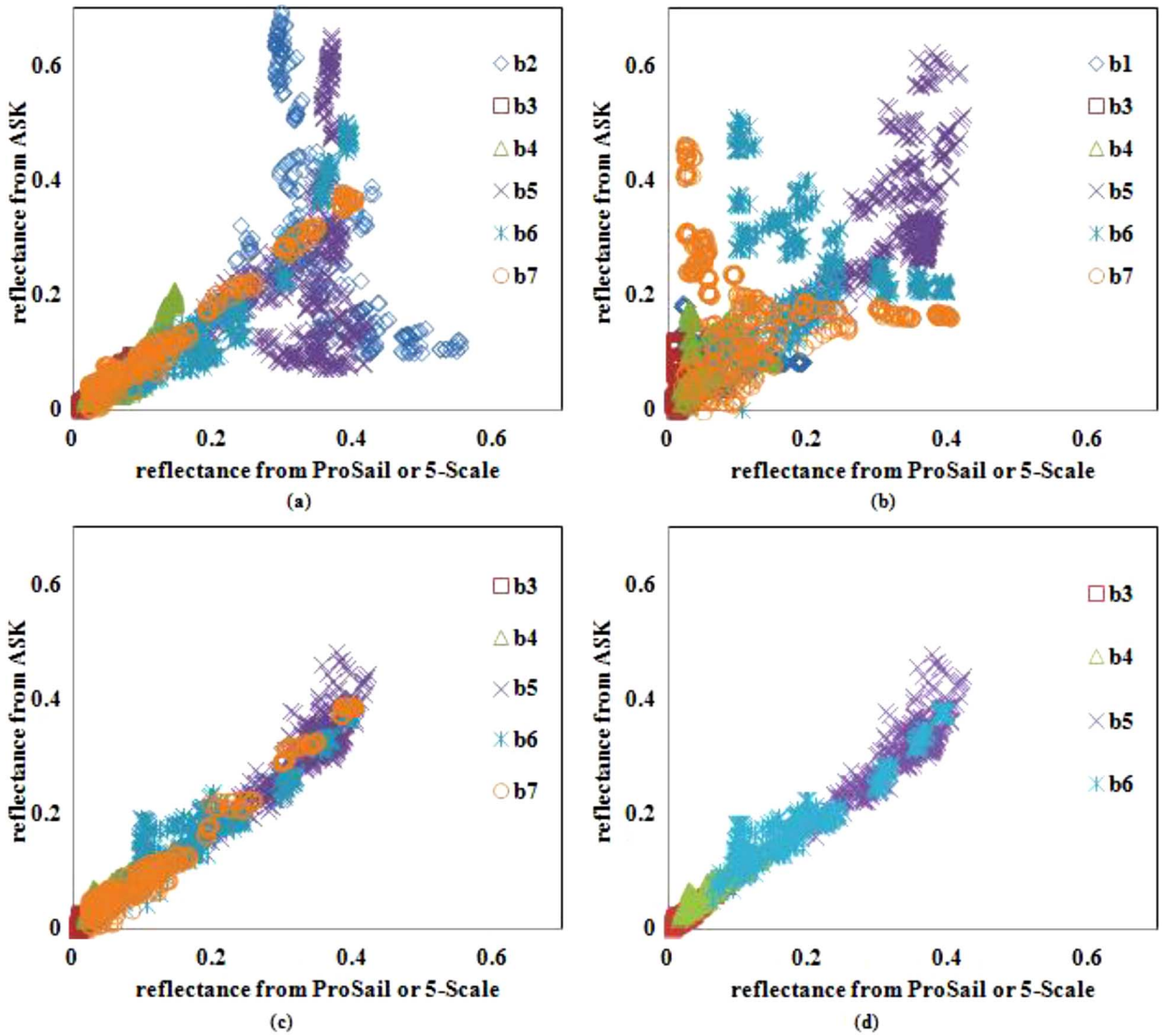

Fig. 11. BRF fitting with different band combinations for retrieval: (a) band1, (b) band2, (c) band1+2, (d) band 1+2+7.

TABLE IV
RMSE FOR BAND BRF FITTINGS WITH DIFFERENT BAND COMBINATIONS FOR RETRIEVAL

band	band1	band2	band3	band4	band5	band6	band7
band1	——	0.2553	0.0056	0.0262	0.1736	0.0572	0.0193
band2	0.0794	——	0.0423	0.0576	0.0854	0.1597	0.1894
band1+2	——	——	0.0051	0.0141	0.0353	0.0341	0.0175
band1+2+7	——	——	0.0051	0.0144	0.0329	0.0289	——

RMSE is approximately 0.023. Adding band3 and band4 to the inversion improves the fitting very slightly, as the RMSEs in b123 and b124 are almost equal to that of b12. This result is can also be seen by comparing b123567 to b1234567 in Fig. 12. The RMSE of b123567 and b124567 are very similar to that of b1234567, indicating that band3 and band4 make little contribution to the inversion accuracy. However, the conditions for SWIR are completely different. When one of the SWIR bands is combined, the accuracy is improved obviously; the RMSEs of b125, b126 and b127 decrease by nearly 0.003–0.004 compared to b12. The cause of this difference may be the numerical correlation among bands, which is discussed in Section III-C.2.

IV. SYNERGISTIC RETRIEVAL OF ALBEDO COMBINING MULTI-SENSORY DATA IN THE HEIHE RIVER BASIN

The study region is located in the Heihe River Basin, which features fairly homogeneous geography and variable landscapes, e.g., barrens, desert, the Gobi desert, and crop lands.

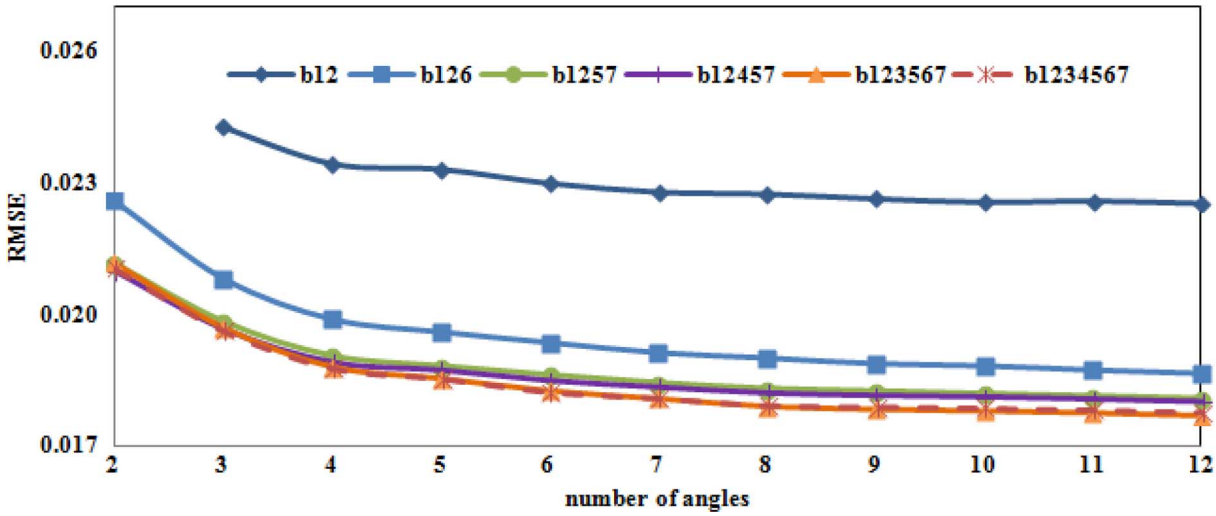

Fig. 12. RMSE of BRF fitting by ASK retrieved under different situations.

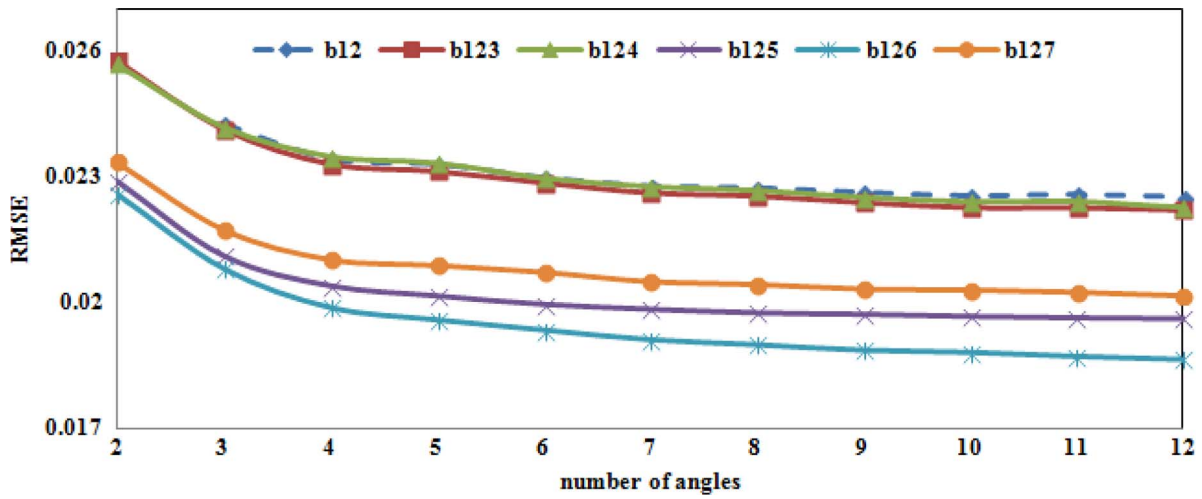

Fig. 13. RMSE of BRF fitting by ASK retrieved using a 3-band combination comparing to b12.

The retrieval albedo is directly compared with the ground measurements, which are provided by the experiment carried out in Heihe from July to August 2011. For each land cover type, the corresponding components spectra input are the typical spectra collected in the local area during the experiment. For example, in 'YK corn site', the corn spectra and the soil spectra in YK are collected as priori-knowledge; for 'BDK site' which is covered by rape flowerer, the rape flowerer spectra is obtained there (YK corn site and BDK site are the validation sites). In addition, the shortwave albedo is interpolated between the shortwave BSA and shortwave WSA with the diffuse skylight factor simulated by the 6S with field-measured aerosol optical depth and water vapor. For quality control, the clear-sky data are selected. The retrieval flow chart is shown as in Fig. 14. The results are validated directly with the *in situ* albedo, where the sites are selected with plot-level measurements over 3×3 km homogeneous quadrates of a land cover.

Fig. 15 compares the satellite retrievals and *in situ* albedo, and the detailed information is listed in Table V. Table VI shows the number of clear sky images obtained in the 4-day composite resolution retrieval. The results retrieved by 8-day composited FY3/VIRR + AVHRR data, as shown as Fig. 15(a), have accuracy similar to the MCD43 product in Fig. 15(b), where the RMSE are 0.0217 and 0.0211, respectively. However, the total observations of the FY3/VIRR and AVHRR during the 16-day accumulation to composite the 8-day temporal resolution are less than those of MODIS (including Terra and Aqua), as shown in Table VI. The composited dates are set to those of the MCD43, and our data processing ended on August 31st; thus, the last inversion period of the 8-day composition ended on the 31st, corresponding to fewer observation dates relative to its MCD43 counterpart. However, the retrieval error (from 20120821 to 20120827) is comparable to that of the MCD43, indicating that the ASK model needs fewer angular samplings to achieve good inversion than the traditional kernel-driven model. Even if the data accumulation period is shortened to 4 days, the albedo retrieved by combining FY3/VIRR and AVHRR, as shown in Fig. 15(c), are almost the same as the 8-day composite results with a slightly higher of RMSE 0.0224. More strongly scattered albedo are seen in Fig. 15(c), appearing outside the bias range of $[-0.015, 0.015]$. However, they still are within the accuracy limit of 0.05. Furthermore, with the MODIS re-

TABLE V
VALIDATION OF RETRIEVED ALBEDO

Date	Site name	Lon/Lat	*in situ*	Case 1	Case 2	Case 3	MCD43
20110725	JC Barrens	100.70°E/ 38.75°N	0.1555	0.1488	0.1446	0.1504	0.1561
20110729	HZZ Barrens	100.32°E/ 38.76°N	0.1872	0.1676	0.1602	0.1709	0.1768
20110808	HZZ Barrens	100.32°E/ 38.76°N	0.1857	0.1633	0.1633	0.1792	0.1757
20110809	BJ Barrens	100.26°E/ 38.93°N	0.2254	0.1763	0.1763	0.2080	0.2066
20110811	HPX Barrens	100.47°E/ 38.72°N	0.1988	0.1664	0.1664	0.1886	0.1924
20110821	JC Barrens	100.70°E/ 38.75°N	0.1462	0.1620	0.1342	0.1577	0.1594
20110822	JC Barrens	100.70°E/ 38.77°N	0.1641	0.1622	0.1328	0.1559	0.1526
20110824	HZZ Barrens	100.32°E/ 38.76°N	0.1689	0.1877	0.1571	0.1709	0.1693
20110825	HPX Barrens	100.47°E/ 38.71°N	0.2155	0.2092	0.2030	0.2046	0.1967
20110827	HZZ Barrens	100.32°E/ 38.76°N	0.1930	0.1877	0.1847	0.1807	0.1693
20110828	JC Barrens	100.70°E/ 38.75°N	0.1700	---	0.1646	0.1645	0.1554
20110802	EG Gobi	100.91°E/ 42.07°N	0.2056	0.1988	0.2389	0.2256	0.2083
20110803	EG Gobi	101.15°E/ 42.38°N	0.2113	0.1755	0.1871	0.2044	0.2032
20110806	HC Gobi	100.92°E/ 41.61°N	0.1907	0.2084	0.2084	0.2053	0.1791
20110726	BDK Rapeflower	101.10°E/ 38.22°N	0.2301	0.2471	0.2221	0.2360	0.1939
20110822	BDK Rapeflower	101.08°E/ 38.26°N	0.2119	0.2090	0.2081	0.1841	0.1729
20110824	YK Corn	100.41°E/ 38.86°N	0.1778	0.2083	0.1535	0.1590	0.1562
20110731	Dz Desert	100.56°E/ 38.50°N	0.1715	0.1772	0.1702	0.1773	0.1841
20110805	EG Saline alkali soil	100.71°E/ 42.21°N	0.2385	0.2436	0.1903	0.2409	0.1903

Case 1 comprises the results retrieved by ASK, combining FY3/VIRR and AVHRR in a composited 8-day cycle. Case 2 comprises the results of combining the two-sensor data in a composited 4-day period. Case 3 comprises the results combining the FY3/VIRR, AVHRR and MODIS sensor data in a 4-day resolution. The retrieved albedo of case 1 and case 2 are the same for the dates from 20110808 to 20110811.

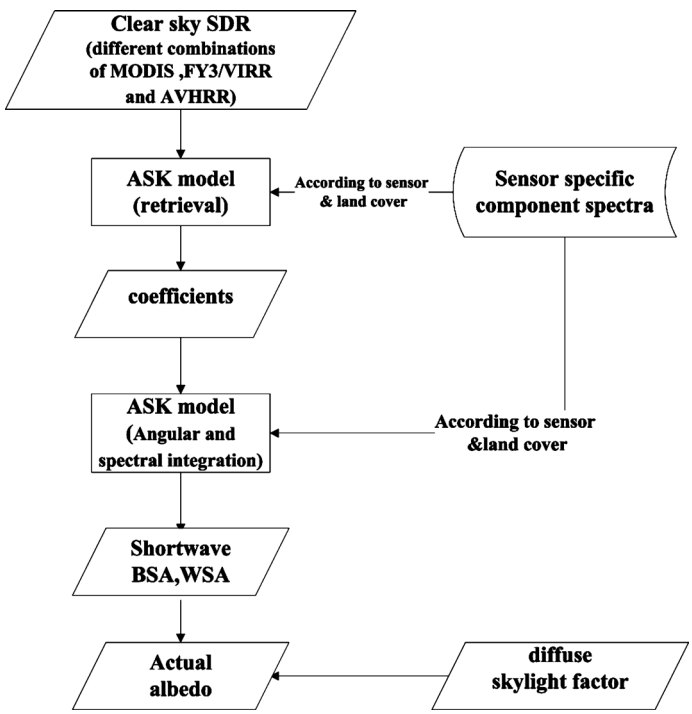

Fig. 14. The flow chart of the albedo retrieval from ASK model using different sensor combinations data. SDR is short for land surface directional reflectance, e.g., the atmospheric corrected data.

flectance input to the ASK, the retrieval shows the highest consistence with *in situ* measurements in Fig. 15(d) and its RMSE falls to 0.0131.

Adding MODIS data, which doubles the observation times (shown in Table VI), to expand the angular sampling range clearly improves the retrieval and shortens the inversion period compared to the MCD43 products. This indicates a promising potential for combining multi-sensor data to synergistically retrieve the land surface parameters at a finer temporal resolution, which is meaningful for remote sensing to capture the fast-changing land surface characters.

V. CONCLUSION

This paper presents the performance of the ASK model and its preliminary application to synergistic multisensory retrieval. All the results show the great potential of ASK in BRDF/albedo retrieval with the combination of multiple bands or sensors. The ASK model, combining multiple bands to fit the BRF, requires fewer angles to achieve a stable inversion, e.g., at least four angle samples when combining all seven MODIS bands, whereas the original kernel-driven model requires at least 7 angles. It also has good prediction ability in the spectral dimension, where the red and NIR bands are the very basic inputs for ASK to fit the coefficients. If a SWIR band is added, the ASK controllability improves clearly in the spectral dimension over the entire shortwave domain, unlike band3 or band4. In general, 4 or 5 angles are needed to achieve a stable inversion for these different band combinations where red and NIR are basically required, based on the analysis of seven MODIS bands. Even in poor angular (2 or 3 angles) or spectral samplings (only combining red and NIR bands), ASK still achieves good BRF

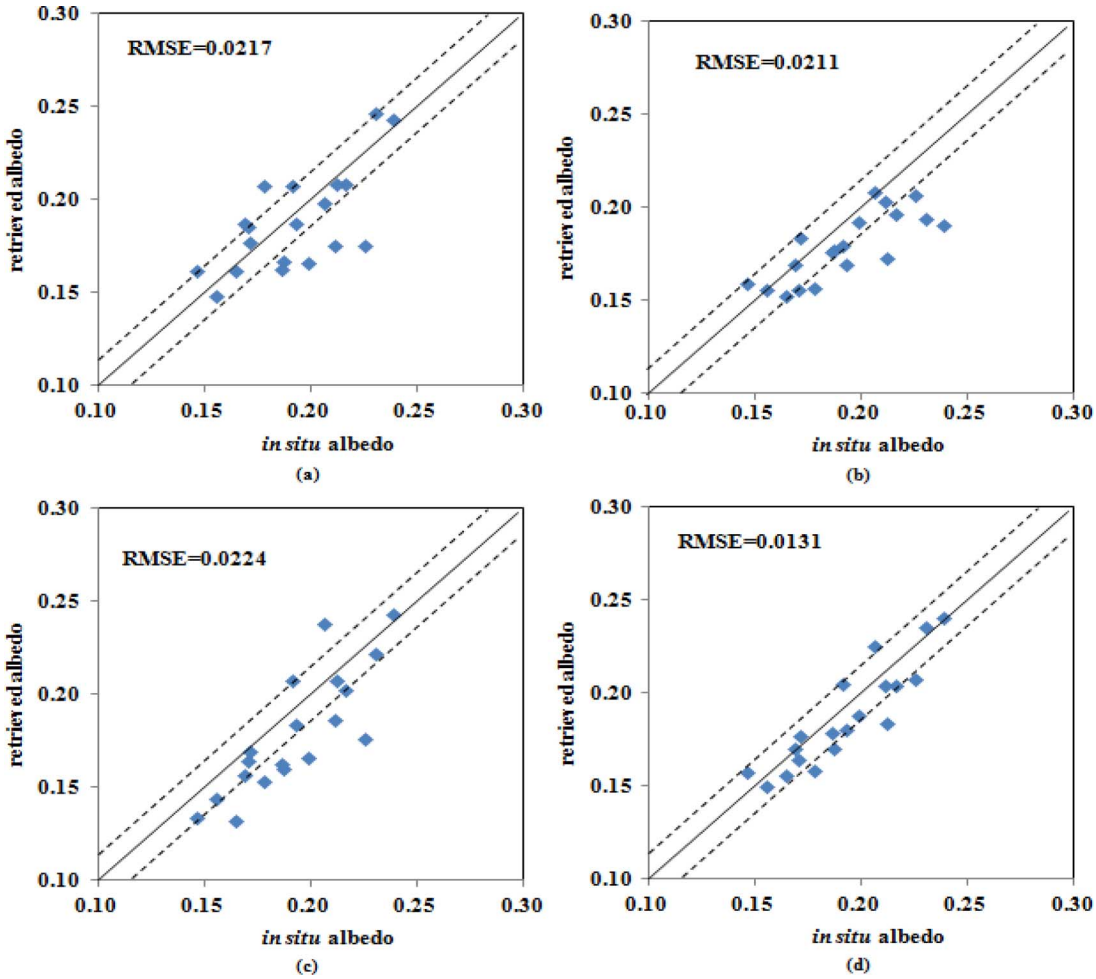

Fig. 15. Validation of satellite albedo retrievals. Panel (a) is the comparison of the retrievals of FY3/VIRR + AVHRR with an 8-day temporal resolution with ground measurements. Panel (b) is the MCD43 albedo. Panel (c) is FY3/VIRR + AVHRR with a 4-day temporal resolution. Panel (d) is FY3/VIRR + AVHRR + MODIS with a 4-day temporal resolution. The two dashed lines in each panel show the bias range between $[-0.015, 0.015]$.

TABLE VI
NUMBER OF CLEAR-SKY IMAGES COLLECTED DURING THE 4-DAY COMPOSITE PERIOD

Period	MODIS	AVHRR	FY3/VIRR
20110724-20110727	8	4	5
20110728-20110731	6	4	3
20110801-20110804	10	5	4
20110805-20110808	12	4	5
20110809-20110812	4	1	1
20110821-20110824	12	4	6
20110825-20110828	12	3	5

fittings. Thus, ASK presents good predicting ability in both the angular and spectral dimensions.

The parameterization of the a priori known component spectra can affect the ASK's inversion accuracy. The average RMSEs of BRF fitting with different component spectra is within 0.02 for albedo. This indicates that the ASK coefficients can be adjusted somewhat to fit the BRF using the inaccurate component spectra, which makes the model robust to the uncertainty from the component spectra.

The synergistic retrieval of albedo in the Heihe River Basin combining MODIS, AVHRR and FY3/VIRR presents a satisfactory consistence with the *in situ* measurements. Combining the AVHRR and FY3/VIRR in an 8-day composited resolution to retrieve ASK yields comparable results to the MCD43 products. Adding the MODIS reflectance data, the accuracy is improved obviously to an RMSE of 0.013, whereas that of the MCD43 is 0.021, despite the use of a shortened 4-day composite temporal resolution.

The ASK model takes advantage of the sensor-dependent component spectra to integrate the multiple bands or multiple sensors to retrieve the BRDF/albedo. Its unique property makes multiple-sensor synergistic retrieval available, which will improve the accuracy and the temporal resolution of the land surface parameter extracted from the remote sensing data. In the application part (chapter IV), the component spectra in Heihe are collected in the local area for those validation sites. However, for global application, a more effective ASK parameterization method is needed to broaden its application. One alternative way is building a component spectra database to obtain the suitable component spectra in operational applications, using the spectra available in common spectral libraries or from field experiments.

ACKNOWLEDGMENT

The authors would like to thank Sihan Liu for the help on the ASK model, Huaguo Huang for the provision of RGM simulated data, and BRDF/Albedo team of the radiation transfer lab in Institute of Remote Sensing and Digital Earth of Chinese Academy of Sciences for the collection and processing of the satellite data and *in situ* data. Also thanks to LOPEX 93 and JHU spectral library for the spectra data, and the MODIS, AVHRR and FY3/VIRR team for the satellite data.

REFERENCES

[1] J. Stroeve *et al.*, "Accuracy assessment of the MODIS 16-day albedo product for snow: Comparisons with Greenland in situ measurements," *Remote Sens. Environ.*, vol. 94, pp. 46–60, 2005.

[2] R. E. Dickinson, "Land processes in climate models," *Remote Sens. Environ.*, vol. 51, pp. 27–38, 1995.

[3] R. B. de Souza *et al.*, "Multi-sensor satellite and in situ measurements of a warm core ocean eddy south of the Brazil-Malvinas Confluence region," *Remote Sens. Environ.*, vol. 100, pp. 52–66, 2006.

[4] S. Liang, "A direct algorithm for estimating land surface broadband albedos from MODIS imagery," *IEEE Trans. Geosci. Remote Sens.*, vol. 41, pp. 136–145, 2003.

[5] J. Wen *et al.*, "Parametrized BRDF for atmospheric and topographic correction and albedo estimation in Jiangxi rugged terrain,," *China. Int. J. Remote Sens.*, vol. 30, pp. 2875–2896, 2009.

[6] W. Lucht, C. B. Schaaf, and A. H. Strahler, "An algorithm for the retrieval of albedo from space using semiempirical BRDF models," *IEEE Trans. Geosci. Remote Sens.*, vol. 38, pp. 977–998, 2000.

[7] F. E. Nicodemus, J. C. Richmond, and J. C. Richmond, "Geometrical considerations and nomenclature for reflectance," U.S. Dept. Commerce, National Bureau of Standards, Washington, DC, USA, 1977.

[8] K. Ranson, J. Irons, and C. Daughtry, "Surface albedo from bidirectional reflectance," *Remote Sens. Environ.*, vol. 35, pp. 201–211, 1991.

[9] B. Pinty *et al.*, "Surface albedo retrieval from Meteosat, 1. Theory," *J. Geophys. Res.*, vol. 105, pp. 099–112, 2000.

[10] A. Strahler *et al.*, "MODIS BRDF/albedo product: algorithm theoretical basis document version 5.0," MODIS documentation, 1999.

[11] C. B. Schaaf *et al.*, "First operational BRDF, albedo nadir reflectance products from MODIS," *Remote Sens. Environ.*, vol. 83, pp. 135–148, 2002.

[12] M. Leroy *et al.*, "Retrieval of atmospheric properties and surface bidirectional reflectances over land from POLDER/ADEOS," *J. Geophys. Res.*, vol. 102, pp. 17023–17037, 1997.

[13] O. Hautecœur and M. Leroy, "Surface bidirectional reflectance distribution function observed at global scale by POLDER/ADEOS," *Geophys. Res. Lett.*, vol. 25, pp. 4197–4200, 1998.

[14] B. Geiger *et al.*, "Product user manual (PUM) land surface albedo," p. 41, LSA SAF internal documents, 2005.

[15] B. Geiger, O. Hagolle, and P. P. Bicheron, "ATBD-WP1130 version 2.0 CYCLOPES-ATBD directional normalisation," 2005.

[16] R. Lacaze, "CSP—Algorithm theoretical basis document (ATBD) WP 8312—Customisation for LAI, fAPAR, fcover and albedo," 2004, (Issue 1.00).

[17] S. Ganguly *et al.*, "Generating vegetation leaf area index earth system data record from multiple sensors. Part 1: Theory," *Remote Sens. Environ.*, vol. 112, pp. 4333–4343, 2008.

[18] E. Vermote and N. Saleous, "Calibration of NOAA16 AVHRR over a desert site using MODIS data," *Remote Sens. Environ.*, vol. 105, pp. 214–220, 2006.

[19] B. Tan *et al.*, "The impact of gridding artifacts on the local spatial properties of MODIS data: Implications for validation, compositing, and band-to-band registration across resolutions," *Remote Sens. Environ.*, vol. 105, pp. 98–114, 2006.

[20] S. Liu *et al.*, "The angular and spectral kernel model for BRDF and albedo retrieval," *IEEE J. Sel. Topics Appl. Earth Observ.*, vol. 3, pp. 241–256, 2010.

[21] R. Deng *et al.*, "Research on remote sensing model for soil water on rough surface," *J. Remote Sens. (China)*, vol. 18, pp. 75–80, 2004.

[22] W. Verhoef, "Light scattering by leaf layers with application to canopy reflectance modeling: The SAIL model," *Remote Sens. Environ.*, vol. 16, pp. 125–141, 1984.

[23] S. Jacquemoud and F. Baret, "PROSPECT: A model of leaf optical properties spectra," *Remote Sens. Environ.*, vol. 34, no. 2, pp. 75–91, 1990.

[24] J. M. Chen and S. G. Leblanc, "A four-scale bidirectional reflectance model based on canopy architecture," *IEEE J. Sel. Topics Appl. Earth Observ.*, vol. 35, pp. 1316–1337, 1997.

[25] T. P. P. Dawson, P. P. J. Curran, and S. E. Plummer, "LIBERTY—Modeling the effects of leaf biochemical concentration on reflectance spectra," *Remote Sens. Environ.*, vol. 65, pp. 50–60, 1998.

[26] Q. Liu *et al.*, "An extended 3-D radiosity-graphics combined model for studying thermal-emission directionality of crop canopy," *IEEE J. Sel. Topics Appl. Earth Observ.*, vol. 45, pp. 2900–2918, 2007.

[27] E. Vermote and A. Vermeulen, "Atmospheric correction algorithm: Spectral reflectances (MOD09)," MODIS ATBD Version 4.0, 1999 [Online]. Available: http://mod09val.ltdri.org/publications/atbd_mod09.pdf

[28] B. Hosgood *et al.*, "Leaf Optical Properties Experiment 93 (LOPEX93)," European commission, Ispra, Italy, 1995 [Online]. Available: ftp://139.191.1.93/verstmi/lopex/LOPEX93D.pdf

[29] W. Wanner, X. Li, and A. Strahler, "On the derivation of kernels for kernel-driven models of bidirectional reflectance," *J. Geophys. Res.*, vol. 100, pp. 21077–21090, 1995.

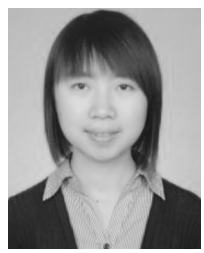

Dongqin You received the B.A. degree from Beijing Normal University, Beijing, China, in 2010. She is currently studying for the Ph.D. degree at the Institute of Remote Sensing and Digital Earth, Chinese Academy of Sciences, Beijing. Her study interests are in modeling and retrieving of bidirectional reflectance distribution function and albedo, multi-sensor synergistic application.

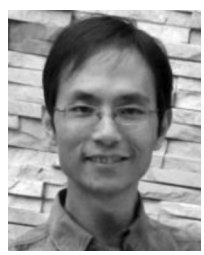

Jianguang Wen received the B.S. degree in geographic information system and the M.S. degree in cartography and geographic information system from Jilin University of China in 2002 and 2005, respectively, and the Ph.D. degree in quantitative remote sensing from the Institute of Remote Sensing Applications, Chinese Academy of Sciences, Beijing, in 2008.

He is currently an Associate Researcher with the Institute of Remote Sensing and Digital Earth, Chinese Academy of Sciences. His main research interest is remote sensing radiative transfer mechanism and inversion, remote sensing experiment in land surface parameters validation.

Qiang Liu received the B.S. degree in computational mathematics from Beijing University, Beijing, China, in 1997 and the Ph.D. degree in cartography and remote sensing from the Institute of Remote Sensing Applications, Chinese Academy of Sciences, Beijing, in 2002.

From 2002 to 2009, he was an Assistant Researcher and later an Associate Researcher with the Institute of Remote Sensing Applications, Chinese Academy of Sciences. Since 2009, he has been a Senior Researcher with the College of Global Change and Earth System Science Beijing Normal University, Beijing Normal University, Beijing, China. He is also a member in the State Key Laboratory of Remote Sensing Science, jointly supported by the Institute of Remote Sensing and Digital Earth, Chinese Academy of Sciences and Beijing Normal University. His main research interest is multi-angular remote-sensing modeling and inversion, with applications in agriculture, ecosystems, and forest studies.

Qinhuo Liu (M'97) received the B.Sc. degree in hydrogeology and engineering geology from Southwest Jiaotong University, Chengdu, Sichuan, China, in 1988, and the M.Sc. degree in cartography and remote sensing and the Ph.D. degree in atmospheric physics from Peking University, Beijing, China, in 1994 and 1997, respectively.

He was a Post-doc since 1997 to 1999 and a Researcher from 1999 to 2012 with the Institute of Remote Sensing Applications, Chinese Academy of Sciences. He visited INRA of France in 1998, Boston University in 1999, University of Maryland in 2003, and George Mason University in 2011 as a Visiting Scholar. He is currently a Researcher and the Deputy Director of the State Key Laboratory of Remote Sensing Science, Institute of Remote Sensing and Digital Earth, Chinese Academy of Sciences, Beijing, China. His research interests focus on remote sensing monitoring for the land surface energy balance, including radiation transfer modeling, inversion and assimilation.

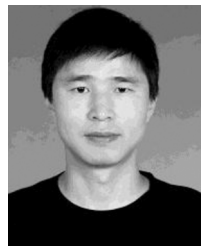

Yong Tang received the B.S. degree in hydrology and water resources from Nanjing University of China in 1997, and the M.S. degree in cartography and remote sensing from the Institute of Remote Sensing Applications, Chinese Academy of Sciences, Beijing, in 2004.

He is currently an Assistant Researcher with the Institute of Remote Sensing and Digital Earth, Chinese Academy of Sciences. His main research interest is multi-angular remote sensing inversion with applications in agriculture and forest studies.